crystals

MDPI

Article

Binding Strength and Hydrogen Bond Numbers between COVID-19 RBD and HVR of Antibody

Ryan Taoran Wang [1,†], Alex Fan Xu [1,†], Qi Zhou [2], Tinglu Song [3], Kelvin J. Xu [4] and Gu Xu [1,*]

[1] Department of Materials Science and Engineering, McMaster University, Hamilton, ON L8S4L8, Canada; wangt41@mcmaster.ca (R.T.W.); xuf21@mcmaster.ca (A.F.X.)
[2] Department of Health Research Methods, Evidence and Impact, Faculty of Health Sciences, McMaster University, Hamilton, ON L8S4L8, Canada; qzhou@mcmaster.ca
[3] School of Materials Science & Engineering, Beijing Institute of Technology, Beijing 100081, China; song@bit.edu.cn
[4] Fu Foundation School of Engineering and Applied Science, Columbia University, New York, NY 10027, USA; xu.kelvin@columbia.edu
* Correspondence: xugu@mcmaster.ca
† First author.

Abstract: The global battle against the COVID-19 pandemic relies strongly on the human defense of antibody, which is assumed to bind the antigen's receptor binding domain (RBD) with its hypervariable region (HVR). Due to the similarity to other viruses such as SARS, however, our understanding of the antibody-virus interaction has been largely limited to the genomic sequencing, which poses serious challenges to containment and rapid serum testing. Based on the physical/chemical nature of the interaction, infrared spectroscopy was employed to reveal the binding disparity, the real cause of the antibody-virus specificity at the molecular level, which is inconceivable to be investigated otherwise. Temperature dependence was discovered in the absorption value from the 1550 cm^{-1} absorption band, attributed to the hydrogen bonds by carboxyl/amino groups, binding the SARS-CoV-2 spike protein and closely resembled SARS-CoV-2 or SARS-CoV-1 antibodies. The infrared absorption intensity, associated with the number of hydrogen bonds, was found to increase sharply between 27 °C and 31 °C, with the relative absorbance matching the hydrogen bonding numbers of the two antibody types (19 vs. 12) at 37 °C. Meanwhile, the ratio of bonds at 27 °C, calculated by thermodynamic exponentials, produces at least 5% inaccuracy. Beyond genomic sequencing, the temperature dependence, as well as the bond number match at 37 °C between relative absorbance and the hydrogen bonding numbers of the two antibody types, is not only of clinical significance in particular but also as a sample for the physical/chemical understanding of vaccine–antibody interactions in general.

Keywords: COVID-19; spike-antibody interaction; temperature influence

Citation: Wang, R.T.; Xu, A.F.; Zhou, Q.; Song, T.; Xu, K.J.; Xu, G. Binding Strength and Hydrogen Bond Numbers between COVID-19 RBD and HVR of Antibody. *Crystals* **2021**, *11*, 997. https://doi.org/10.3390/cryst11080997

Academic Editor: Vijay S. Reddy

Received: 21 July 2021
Accepted: 19 August 2021
Published: 21 August 2021

1. Introduction

The ongoing battle against the coronavirus (COVID-19, or SARS-CoV-2) has largely been defined by the human antibody, including vaccine development, and rapid diagnosis of serum, all based on the match and binding between its hypervariable region (HVR) and the antigen's receptor binding domain (RBD) [1–8]. However, existing knowledge has been confined by the conflicting observations beyond genomic sequencing, such as the early disappearance of the antibody, which poses serious challenges to the current state-of-the-art COVID-19 IgM/IgG rapid serum tests [9], due in part to the similarity to other viruses, such as SARS and even that of a common flu [10,11]. As a result, the performance of various antibody tests was undesirable [12]. Studies showed that the accuracy of various antibody tests were found to range from 62% to 95% [13,14]. All this indicated that the pandemic might become seasonal, when the current lockdown in some countries failed to stop the spreading of the virus completely [15], and the rapid serum testing was deemed unreliable.

To unravel the cause of the conflicting observations relevant to the RBD and HVR binding, it is necessary to first differentiate the binding variation between SARS-CoV-2 and other less distinguishable coronaviruses, such as SARS-CoV-1, especially in terms of the chemical bonding numbers between the viruses and their respective antibodies [3,16]. In particular, one has to clarify how the binding sites of the spike proteins (S proteins), which are the foremost weapon head of the virus, interact with the antibodies of SARS-CoV-2 (antibody 2), the frontier human defense [3,17,18]. Although a number of characterization methods have already been employed to analyze the structure of the coronaviruses, especially their S proteins [19–21], it was found that the RNA sequence of SARS-CoV-2 bears 89.1% resemblance to SARS-CoV-1 [20], which only deciphers the similar 3D structures of the S proteins between the two viruses obtainable from Cryo-EM [19]. It does not, however, provide the details of the binding disparity between the viruses and their antibodies. Neither could the latter be elucidated by the amino acid sequencing of the S proteins [3,18], despite the finding that 77% of the amino acid sequences were identical in the RBD. Consequently, the attempt thus far has been destined to be less than successful, due not least to the lack of probing of the binding difference between the viruses and their antibodies. More precisely, even the bonding nature between the two has yet to be illustrated, let alone the influence of other factors, such as temperature or the possible antibody dependent enhancement. Thus, it is necessary to reveal the binding details between the spike protein and antibodies at the molecular level, which is less likely to be affected by the complex physiological environment of infected cells.

It is therefore the purpose of the current paper to probe the binding strength variation between the SARS-CoV-2 spike protein/SARS-CoV-2 antibody and SARS-CoV-2 spike protein/SARS-CoV-1 antibody, the closest in genomic sequence. Although the spike protein showed various conformations, among which the RBD structure varies, it is precisely the very reason that we have to study such interactions at the physical level, as the binding consists of a van der Waals force, which has to be probed by vibrational spectroscopies. As speculated, the virus interacts, at the molecular level, with either the IgM/IgG or ACE2, mainly through the hydrogen bonds formed by carboxyl and/or amino groups [22–24]; infrared spectroscopy (FTIR) should thus be the most revealing physical instrument [6,25,26] to probe not only the bonding chemistry in a qualitative manner but also the quantitative information, such as the number of the binding sites, leading to a direct measure of the virus attacking intensity. Employing FTIR, it was found by surprise that the bonding numbers of the two antibody types are almost identical at lab/room temperature or anything below 27 °C. As a result, the antibodies were, astonishingly, rather nonspecific, resulting in a lower than 95% accuracy. On the other hand, such specificity to the SARS-CoV-2 antibody could be achieved at the human body temperature of 37 °C, or at least beyond 31 °C, when the quaternary protein structure would be further unfolded to match that of the antibodies specifically, where the two antibody types reached corresponding numbers of available hydrogen bonds (19 vs. 12) in their structures. Our results undoubtedly call for the necessity of simulating human body temperature in future antibody diagnosis, especially during the search for vaccines, as the binding uniqueness, or the specificity of SARS-CoV-2 IgM/IgG, could only be fully obtainable at a warmer temperature, rather than under the usual lab/room temperature of 20–25 °C, where most of the vaccine research is conducted [27].

2. Experimental Procedure

SARS-CoV-2 spike RBD-His (V367F) recombinant protein (Purity: >95% as determined by SDS-Page, protein concentration: 0.1 wt%), SARS-CoV-2 antibody (antibody 2, also named SARS-CoV-2 (2019-nCoV) spike Neutralizing Antibody), and SARS-CoV-1 antibody (antibody 1, also named SARS-CoV/SARS-CoV-2 spike S1 antibody) (Purity: >95% as determined by SDS-Page, protein concentration: 0.1 wt%) were all purchased from Sino Biological Inc., Chesterbrook, PA, USA. PBS solution (phosphate buffered solution contain-

ing 0.1 wt% NaCl + 0.002 wt% KCl + 0.01 wt% Na_2HPO_4 + 0.002 wt% KH_2PO_4 + 99$^+$ wt% H_2O) was purchased from Solarbio Corp, Pasig, Philippines.

A Nicolet iS50 FT-IR spectrometer (Thermo Fisher Scientific, Massachusetts, U.S.) was adopted to acquire the FTIR spectra, in wavenumber range of 500–4000 cm^{-1} by the attenuated total reflectance (ATR) mode. Samples were placed in a sample stage made of quarts. The specified wavenumber precision is 0.5 cm^{-1} and that of the absorbance is 0.1%. A blank run was first conducted to ensure the calibration. An electric heating element was installed to change the temperature of the sample stage. The temperature was recorded via electronic thermometer with an accuracy of ±0.1 °C. The liquid samples were pipetted to ensure the same amount of 3 μL each time.

The acquired FTIR data were inverted to obtain the % absorption from (100%-trans mittance %). PBS solvent contributions can be eliminated by subtracting the spectra of PBS under identical conditions. Infrared absorption at 750 cm^{-1} and 1550 cm^{-1} was determined by the difference between the crest and the trough. The associated error bars were estimated by adding the instrumental error (0.1%, as has been indicated in the apparatus manual), the possible deviation involved in the computation, and the standard deviation of several repeating measurements.

3. Results and Discussion

Based on the nature of hydrogen bonding between the pairs of carboxyl and amino groups (Figure 1a), samples of antibodies and spike proteins were mixed and underwent FTIR spectroscopic examination conditioned by variable temperature (Figure 1b). As the protein sample concentrations are quite low (0.1 wt%), the attenuated total reflectance (ATR) type of FTIR has been adopted, which entertains a tiny sample amount of several microliters, 0.1% error margin in the absorption measurement, and 0.5 cm^{-1} along the wavenumber scan. To facilitate the possible temperature variation, an electric heating element and a thermometer were attached to the metallic plate of the ATR assembly, which also acts as an ideal heat sink (Figure 1b). To include all the possible hydrogen bond stretching modes (Figure 1a), the entire mid infrared spectrum was scanned for the two 1:1 mixtures of SARS-CoV-2 spike protein/SARS-CoV-2 antibody (S + Antibody 2) and SARS-CoV-2 spike protein/SARS-CoV-1 antibody (S + Antibody 1) (Figure 1c,d), where many absorption bands are observed which could be attributed to the proteins, such as: 2500–3500 cm^{-1} from –OH, 2400–3200 cm^{-1} from NH_2, 1650 cm^{-1} from the peptide bonds, and 800–1000 cm^{-1} from C–H [6]. However, due to the low concentration, they are mostly overlapped by the FTIR of the buffer solution PBS, which is dominated by water (0.1 wt% NaCl + 0.002 wt% KCl + 0.01 wt% Na_2HPO_4 + 0.002 wt% KH_2PO_4 + 99$^+$ wt% H_2O), such as: 2500–3500 cm^{-1} from –OH stretching, 2250–2500 cm^{-1} from H–O–H bending, 1650 cm^{-1} from –OH scissoring, and 800–1000 cm^{-1} from H_2O liberation, which could not be easily resolved by D_2O replacement, [28,29] although the absorption band at around 1630 cm^{-1} does show some protein variation [6]. Fortunately, there exists an FTIR absorption band exclusively associated with the proteins but not overshadowed by the solvent at 1550 cm^{-1} (Figures 1c–d and 2a,b), which is caused by the carboxyl and amino groups in the amino acid [30], allowing us to probe the protein bonding variation.

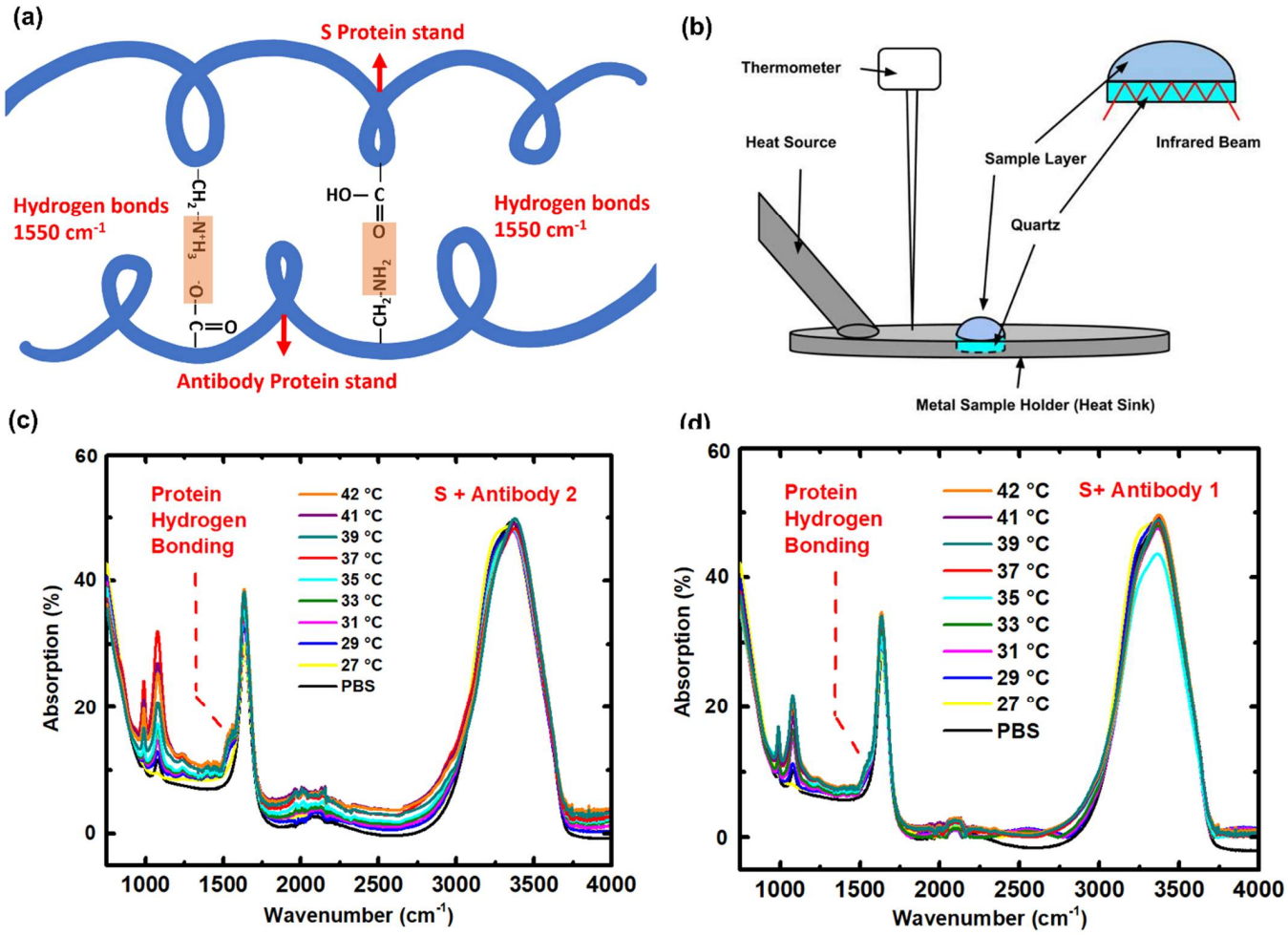

Figure 1. (**a**) Schematic illustration of the hydrogen bonding between carboxyl and amino groups of the protein strands, representing a typical intermolecular binding for the secondary structure of proteins. (**b**) For the FTIR apparatus, the ATR model has been adopted to improve the signal noise ratio, which offers 0.1% error margin in the absorption measurement and 0.5 cm^{-1} along the wavenumber scan. To facilitate the possible temperature variation, an electric heating element and a thermometer were attached to the metallic plate of the ATR assembly, which also acts as an ideal heat sink. Samples of antibodies and spike proteins were mixed together and underwent FTIR spectroscopic examination conditioned by variable temperatures. (**c**) The FTIR scan of the sample mixture of SARS-CoV-2 spike protein/SARS-CoV-2 antibody (S + Antibody 2) in PBS solution. Comparing the FTIR signal of the PBS solvent, it indicates that 1550 cm^{-1} was the only absorption band exclusively associated with the proteins but not overshadowed by the PBS solvent. (**d**) The same FTIR scan of the sample mixture of SARS-CoV-2 spike protein/SARS-CoV-1 antibody (S + Antibody 1) in PBS solution.

More details can be found in Figure 2a,b, where a strong temperature dependence is observed by surprise (Figure 2c) for the absorption band of 1550 cm^{-1} after the subtraction of the buffer solution absorption. At 27 °C, for example, similar absorbances of 0.5% and 0.4% were found at 1550 cm^{-1} between the mixtures of the SARS-CoV-2 spike protein/SARS-CoV-2 antibody and the SARS-CoV-2 spike protein/SARS-CoV-1 antibody, respectively. However, the absorbance increased to 4.4% and 2.5% at 31 °C, respectively, presenting not only a significant amount of enhancement, but also a 72% discrepancy between the two types of antibodies. The enhanced absorption at 1550 cm^{-1} clearly indicates the augmentation of the hydrogen bonding numbers, rather than strengthening the binding itself, as the latter would relocate the band to a larger wavenumber, corresponding to the higher energy. Therefore, the result implies that there are fewer bonds, or less specificity, between the spike protein and its antibody at lab/room temperature of below 27 °C when the S association with the SARS-CoV-2 antibody and SARS-CoV-1 antibody becomes similar, leading to the possible false conclusion. The difference or specificity will, however, be

enhanced at higher temperatures, at least beyond 31 °C, when the ratio becomes almost 19 vs. 11, effectively suppressing the binding of the wrong types of antibody (Figure 2c).

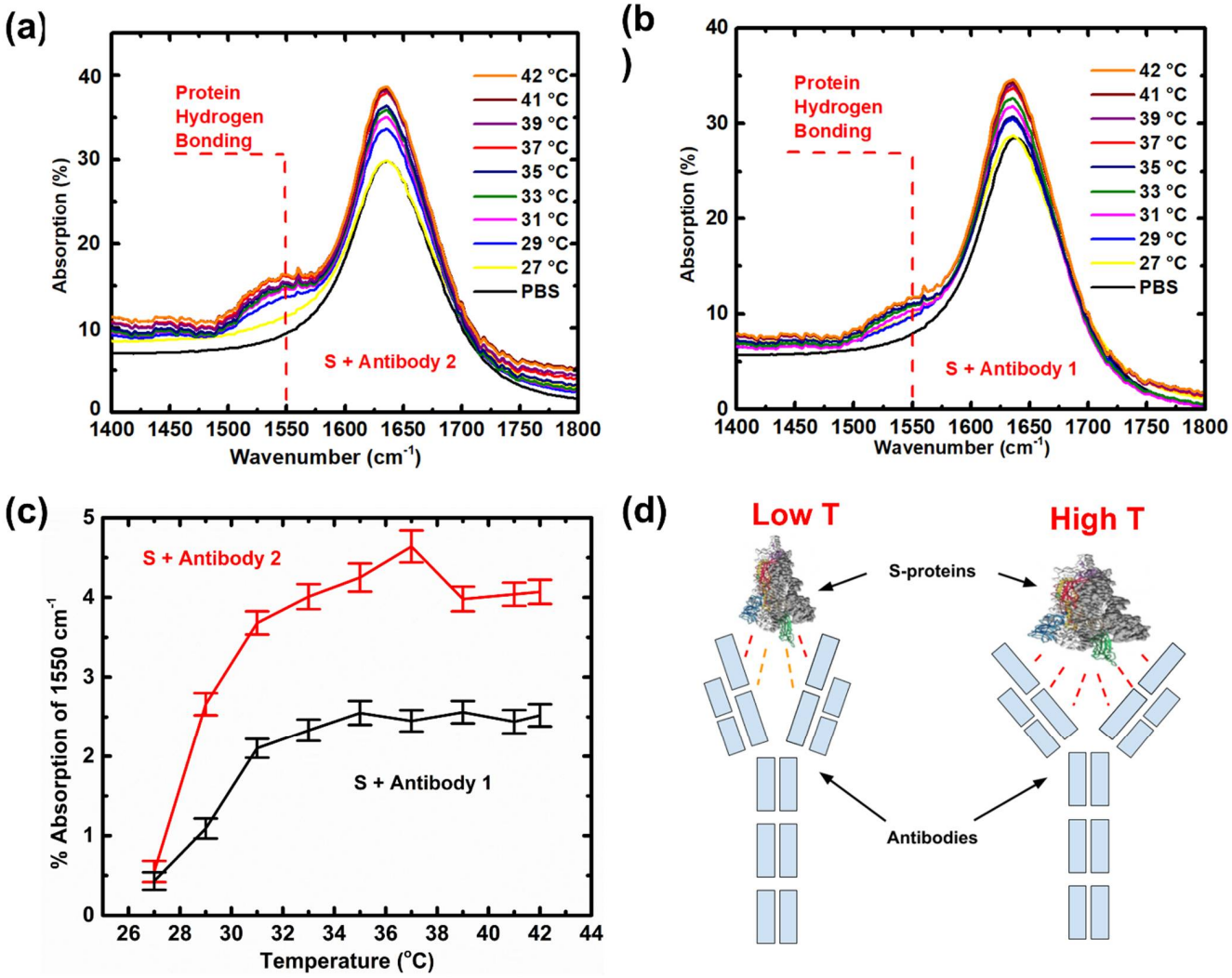

Figure 2. (**a**) Detailed FTIR scan of the sample mixture of SARS-CoV-2 spike protein/SARS-CoV-2 antibody (S + Antibody 2) in PBS solution, within the wavenumber range of 1400–1800 cm^{-1}. (**b**) Detailed FTIR scan of the sample mixture of SARS-CoV-2 spike protein/SARS-CoV-1 antibody (S + Antibody 1) in PBS solution, in the wavenumber range of 1400–1800 cm^{-1}. (**c**) The infrared absorptions of 1550 cm^{-1} under variable temperature of the sample combination of SARS-CoV-2 spike protein/SARS-CoV-2 antibody versus the sample combination of SARS-CoV-2 spike protein/SARS-CoV-1 antibody, obtained from the difference between the peak near 1550 cm^{-1} and the trough near 1480 cm^{-1}, after subtracting that of the buffer solution. The associated error bars were estimated by combining the instrumental error and the possible deviation involved in the computation. A strong temperature dependence is observed, where the bonding number of the antibody is enhanced sharply beyond 31 °C, rather than at the usual room temperature. (**d**) The possible temperature influence on the structure of spike protein and antibodies, where only the top part of the IgM, similar to IgG, was depicted: a higher temperature increases the probability of protein quaternary structure unfolding and exposes more binding sites, hence more bonds.

Such an increase in bonding numbers at elevated temperatures is likely caused by the unfolding of the protein strands (Figure 2d), which can be further verified by Figure 3a–c, where the S proteins and antibodies were assessed by FTIR separately. The absorption band at 1550 cm^{-1} followed a similar trend in temperature (Figure 3d), presumably attributed to the thermal agitation, when the likelihood increases for such binding sites to pair, either between the neighboring proteins or amongst various strands within a protein (Figure 3e). On the other hand, when the spike proteins and antibodies were mixed, the bond pairing occurs mainly across the different species (Figure 1a) in order to obey the

universal law of entropy maximization. The latter can be confirmed by the comparison of Figures 2c and 3d, where the absorbance of the mixture is much larger than the sum of each individual component beyond 31 °C, viz., when the signal would be the average of the two, should there be no mutual interactions, as the samples, or the mixtures, were all prepared by the same 0.1 wt% solutions. In fact, the FTIR contribution caused by the antibody binding to the spikes could be extracted from the difference between the mixture absorption and the superposition of the individual. Beyond the most distinct band at 1550 cm^{-1}, similar trends can also be observed in other absorption bands, such as the 980 cm^{-1} and 1080 cm^{-1}, attributed to –C = O in serine and –OH in threonine [6]. As can be judged from Figures 1–3, both mixture absorptions were similar to the superposition of the individual absorptions at lower temperatures, indicating the relocation of the bond pairing from the individual proteins to the mixtures, whose binding number was relatively small. At higher temperatures, on the other hand, the absorption of both mixtures was much higher than the superposition of the individual absorption, representing a larger binding number. All this can be further verified by an extra absorption band found near 850 cm^{-1}, due exclusively to the binding between the virus spike proteins and the antibodies, since it was absent in the individual spectrum of both viruses.

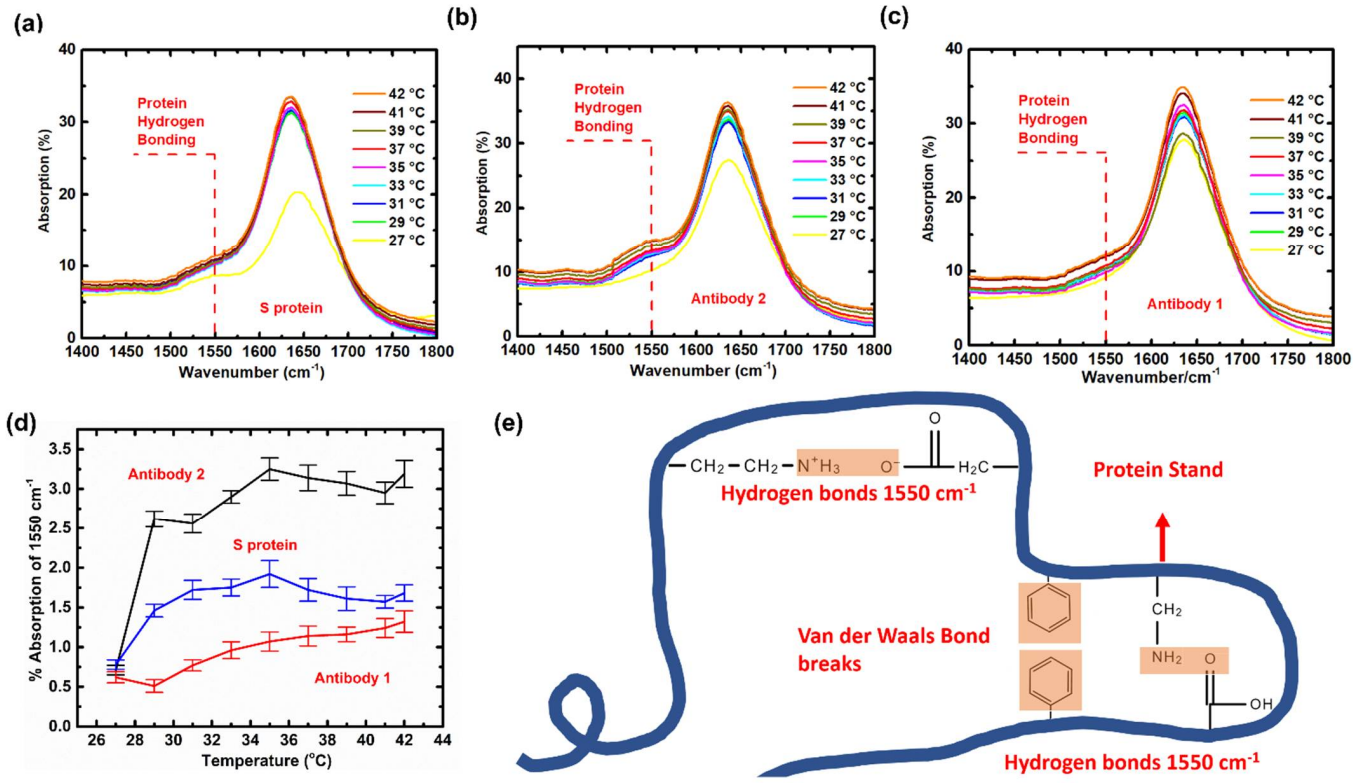

Figure 3. (**a**) The FTIR scan of SARS-CoV-2 spike protein (S protein) in PBS solution for the wavenumber range of 1400–1800 cm^{-1}. (**b**) The FTIR scan of SARS-CoV-2 antibody (antibody 2) in PBS solution for the wavenumber range of 1400–1800 cm^{-1}. (**c**) The FTIR scan of SARS-CoV-1 antibody (antibody 1) in PBS solution for the wavenumber range of 1400–1800 cm^{-1}. (**d**) The infrared absorption of 1550 cm^{-1} under variable temperature of SARS-CoV-2 spike protein, SARS-CoV-2 antibody, and SARS-CoV-1 antibody, respectively, given by the difference between the crest near 1550 cm^{-1} and the trough near 1480 cm^{-1}. The associated error bars were estimated by combining the instrumental error and the possible deviation involved in the computation. All 3 proteins followed a similar trend in temperature, which is attributed to the thermal agitation, when the likelihood increases for such binding sites to pair, either between the neighboring proteins or amongst various strands within a protein or even along a protein strand. (**e**) Schematic illustration of the hydrogen bonding between carboxyl and amino groups within a protein strand, showing the intra-molecular binding of the quaternary structure of proteins when the van der Waals bonds between large pendant groups, such as phenyl, were disrupted, which causes unfolding and exposes more bonding sites.

The gradual exposure of the bonding sites, caused by thermally enhanced unfolding of the quaternary protein structure, was further evidenced by the diminishing van der Waals bonds in the FTIR of spike protein and antibodies, as shown by the 750 cm^{-1} band (Figure 4a–c), which were obtained from the measurement of more concentrated samples via solvent evaporation, to achieve stronger absorption, as well as to reduce the influence of solvent. Being closer to the backbones, the opposite temperature dependence is anticipated for the phenyl groups to the amino/carboxyl groups. Rather than allowing for more hydrogen bonds by the temperature increase, the absorption band of 750 cm^{-1} gradually diminishes at an elevated temperature (Figure 4d), which indicates the collapse of van der Waals bonds between the phenyl groups along the backbone. They must be thermally fractured, allowing the protein strands to further unfold, exposing more hydrogen bonding sites for pairing. The thermally activated unfolding in turn promotes the enhancement in the number of hydrogen bonds between the spike proteins and their antibodies. In the meantime, Figure 4d also verifies the observation by comparing Figures 2c and 3d, viz., the mixing produces more van der Waals bonds due to the entropy maximization, although it occurs at lower temperature for the phenyl groups and does not differentiate the two antibody types. At a higher temperature, this is further escalated between the S protein and the SARS-CoV-2 antibody, due to the hydrogen bonding, as shown in Figure 2c.

As a matter of fact, similar evidence can also be traced from the recent literature, where the binding sites differ between SARS-CoV-2 antibody and SARS-CoV-1 antibody [5,31–33]. For example, amino acid sequencing was conducted for the receptor-binding domains (RBD) of SARS-CoV-2 and SARS-CoV-1 spikes. It was discovered that only 23% of the sequence mismatches between the two spikes, which calls for the further analysis of binding site numbers within this region [18]. From the literature, it was found that there are 19 $–NH_2$ groups and 0 –COOH groups in the side chains of the SARS-CoV-2 spike RBD backbone, whereas their SARS-CoV-1 counterpart contains 11 $–NH_2$ groups and 5 –COOH groups only [18,34]. As these groups form potential binding sites to the antibody, ideally the corresponding SARS-CoV-2 antibody should bear 19 –COOH groups versus the SARS-CoV-1 antibody of only 11 –COOH groups and 5 $–NH_2$ groups (Table 1). This is verified by a recently published paper, which not only confirms the number of hydrogen bonds but also supports the new picture brought together by our results [33].

Table 1. The number of binding sites in SARS-CoV-2/SARS-CoV-1 spike proteins and their antibodies [18,34].

The 23% Region	Number of—NH_2 Group	Number of—COOH Group
SARS-CoV-2 spike sidechains	19	0
SARS-CoV-1 spike sidechains	11	5
SARS-CoV-2 spike antibody [33]	1 (our prediction: 0)	19 (our prediction: 19)
SARS-CoV-1 spike antibody [32]	4 (our prediction: 5)	12 (our prediction: 11)

Further exploring the consequence of the temperature influence on the bonding between virus and antibody, quantitative information may be obtained through the Arrhenius equation, where the probability of bond breaking is related to an exponential function of the bonding energy E over the temperature T: $\exp(-E/RT)$, where R is the gas constant. Such an equation predicts the stability of the protein and the unfolding of the quaternary structures. For example, based on the literature information [8], the possibility to break a hydrogen bond of 19 kJ/mol on the secondary structure is almost negligible (0.04% at 295 K–0.06% at 310 K), whereas a quaternary structure of 1.0–5.0 kJ/mol will much more likely be affected (15–68%) by the same temperature change when more bonding sites on the spike RBD area are exposed, resulting in tighter binding to the antibody. Finally, following thermodynamics, if we designate the bond energy times the number of such bonds per mole for the two antibody types by E_1 and E_2 (kJ/mol), the ratio of bonded antibody numbers, $[Ab_2]/[Ab_1]$, will then be given by $\exp((E_2 - E_1)/RT)$ [35], rather

than the layman's guess of E_2/E_1. Following the result of Figure 2c, where the 0.1% absorbance discrepancy of the two antibodies at 27 °C corresponds to an energy difference of 7.5 KJ/mol, the antibody number ratio can thus be calculated by the exponential to become 20:1, giving rise to 5% of the test uncertainty.

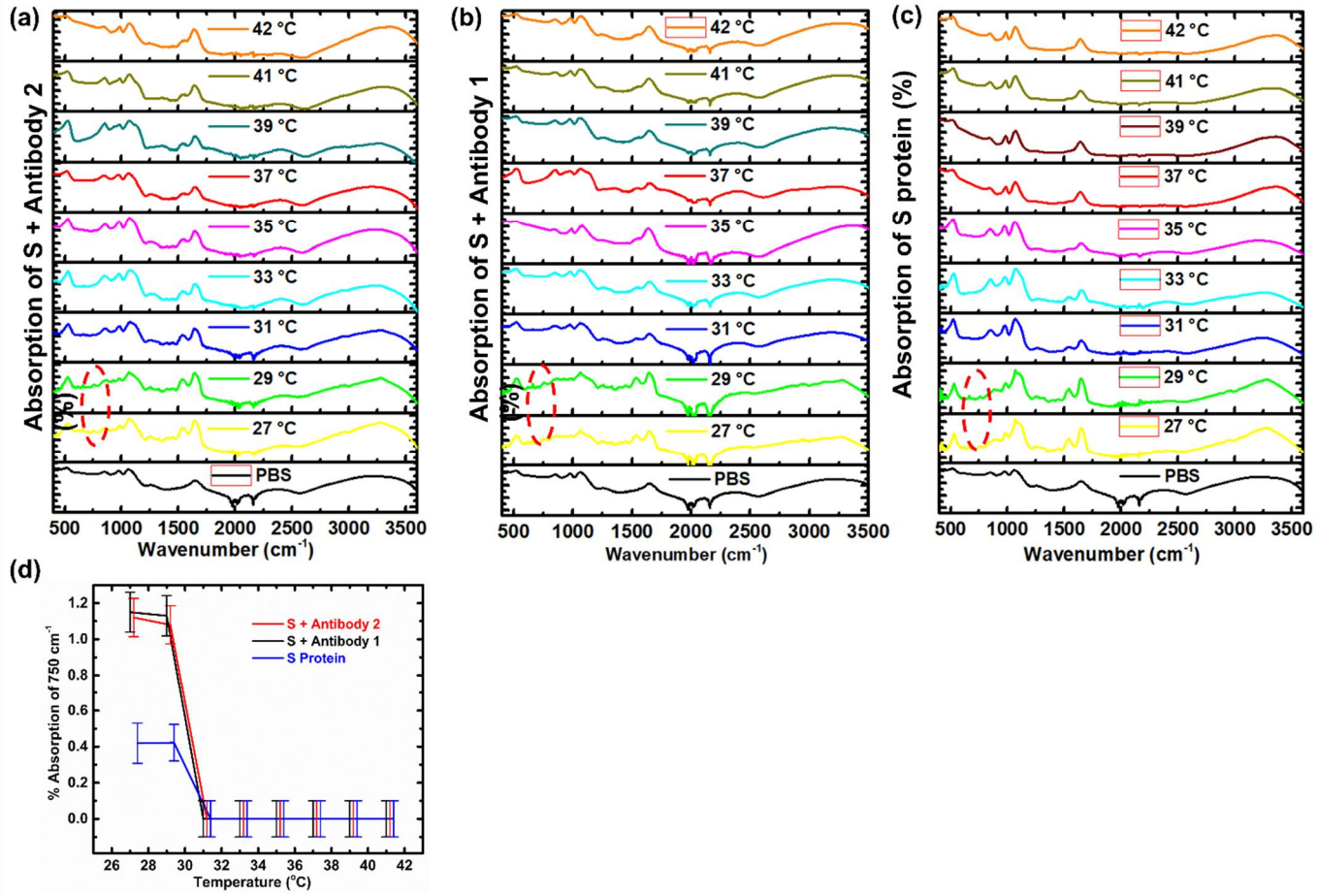

Figure 4. (**a**) The FTIR scan of SARS-CoV-2 spike protein/SARS-CoV-2 antibody (S + Antibody 2), obtained from more concentrated samples, showing visible 750 cm^{-1} bands at 27–29 °C (red circle), exclusively associated with the proteins but not found in the PBS solvent, attributed to the possible van der Waals bonding between the large pendant group such as phenyl. (**b**) Similar FTIR result of SARS-CoV-2 spike protein/SARS-CoV-1 antibody (S + Antibody 1) obtained from more concentrated samples, showing a visible 750 cm^{-1} bands at 27–29 °C (red circle). (**c**) Similar FTIR result of SARS-CoV-2 spike protein alone, obtained from more concentrated samples, showing a visible 750 cm^{-1} bands at 27–29 °C (red circle). (**d**) The infrared absorption of 750 cm^{-1} under variable temperature of SARS-CoV-2 spike protein/SARS-CoV-2 antibody (S + Antibody 2), SARS-CoV-2 spike protein/SARS-CoV-1 antibody (S + Antibody 1), and the spike protein alone, obtained from the difference between the peak near 750 cm^{-1} and the trough near 725 cm^{-1} after subtracting that of the buffer solution. The associated error bars were estimated by combining the instrumental error and the possible deviation involved in the computation.

4. Conclusions

In conclusion, we have further probed interactions between SARS-CoV-2 spike protein and SARS-CoV-2 versus the closest kin of SARS-CoV-1 antibodies. Beyond the usual genomic sequencing, infrared spectroscopic measurement allows us to probe not only the presence of the hydrogen bonds between spike protein and antibodies but also the disparity in the number of bonding sites among the antibodies, given by the thermodynamic exponential ratio. The binding strength between SARS-CoV-2 spike and SARS-CoV-2/SARS-CoV-1 antibodies was found to be temperature dependent, where a higher temperature raises the probability of protein quaternary structure unfolding, which exposes more binding

sites, hence more bond numbers. This was also confirmed by similar observations for the proteins themselves, especially from the diminishing of van der Waals bonds. At the same time, the relative absorbance matches the hydrogen bonding numbers of the two antibody types (19 vs. 11) at 37 °C, whereas the ratio of bonds at 27 °C, calculated by thermodynamic exponentials rather than by the layman's guess, is about 20:1, leading to 95% accuracy at best. Moreover, the virus/antibody bonding specificity is enhanced at human body temperature instead of room temperature, due to the possible protein unfolding by thermal agitation, leading to the necessity of conducting vaccine research at 37 °C to identify various viruses. The temperature variation and the bond numbers not only establish a linkage between the pandemic and molecular level query [36,37] but also provide a new dimension in raising the accuracy of the ongoing rapid antibody test, which will be beneficial to the SARS-CoV-2 vaccine and virus research in general.

Author Contributions: R.T.W. contributed to every stage of the research, A.F.X. performed measurements, K.J.X. helped with manuscript preparation, T.S. supported measurement, Q.Z. assisted the data interpretation, and G.X. initiated and supervised the research. All authors have read and agreed to the published version of the manuscript.

Funding: This research was funded by Natural Sciences and Engineering Research Council of Canada, grant number 10546964 and The APC was funded by Natural Sciences and Engineering Research Council of Canada.

Data Availability Statement: The data underlying this article will be shared on reasonable request to the corresponding author.

Acknowledgments: Thanks are due to the Beijing Institute of Technology for the FTIR support, L. Zhang of University of Toronto Health Network for comments, and J. McLellan of University of Texas at Austin for the artwork of SARS-CoV-2 spike proteins. The NSERC of Canada is also acknowledged.

Conflicts of Interest: The authors declare no conflict of interests.

References

1. Guo, L.; Ren, L.; Yang, S.; Xiao, M.; Chang, D.; Yang, F.; Dela Cruz, C.S.; Wang, Y.; Wu, C.; Xiao, Y.; et al. Profiling early humoral response to diagnose novel coronavirus disease (COVID-19). *Clin. Infect. Dis.* **2020**, *71*, 778–785. [CrossRef]
2. Tang, Y.W.; Schmitz, J.E.; Persing, D.H.; Stratton, C.W. Laboratory diagnosis of COVID-19: Current issues and challenges. *J. Clin. Microbiol.* **2020**, *58*, e00512-20. [CrossRef]
3. Tian, X.; Li, C.; Huang, A.; Xia, S.; Lu, S.; Shi, Z.; Lu, L.; Jiang, S.; Yang, Z.; Wu, Y.; et al. Potent binding of 2019 novel coronavirus spike protein by a SARS coronavirus-specific human monoclonal antibody. *Emerg. Microbes Infect.* **2020**, *9*, 382–385. [CrossRef]
4. Li, Z.; Yi, Y.; Luo, X.; Xiong, N.; Liu, Y.; Li, S.; Sun, R.; Wang, Y.; Hu, B.; Chen, W.; et al. Development and clinical application of a rapid IgM-IgG combined antibody test for SARS-CoV-2 infection diagnosis. *J. Med. Virol.* **2020**, *92*, 1518–1524. [CrossRef] [PubMed]
5. Wang, Q.; Zhang, Y.; Wu, L.; Niu, S.; Song, C.; Zhang, Z.; Lu, G.; Qiao, C.; Hu, Y.; Yuen, K.Y.; et al. Structural and functional basis of SARS-CoV-2 entry by using human ACE2. *Cell* **2020**, *181*, 894–904. [CrossRef] [PubMed]
6. Barth, A. Infrared spectroscopy of proteins. *Biochim. Biophys. Acta (BBA) Bioenerg.* **2007**, *1767*, 1073–1101. [CrossRef] [PubMed]
7. Andersen, N.H. *Protein Structure, Stability, and Folding. Methods in Molecular Biology*; Murphy, K.P., Ed.; Humana Press: Totowa, NJ, USA, 2001; Volume 168.
8. Khalifa, S.A.M.; Yosri, N.; El-Mallah, M.F.; Ghonaim, R.; Guo, Z.; Musharraf, S.G.; Du, M.; Khatib, A.; Xiao, J.; Saeed, A.; et al. Screening for natural and derived bio-active compounds in preclinical and clinical studies: One of the frontlines of fighting the coronaviruses pandemic. *Phytomedicine* **2021**, *85*, 153311. [CrossRef] [PubMed]
9. Roda, A.; Cavalera, S.; Di Nardo, F.; Calabria, D.; Rosati, S.; Simoni, P.; Colitti, B.; Baggiani, C.; Roda, M.; Anfossi, L. Dual lateral flow optical/chemiluminescence immunosensors for the rapid detection of salivary and serum IgA in patients with COVID-19 disease. *Biosens. Bioelectron.* **2021**, *172*, 112765. [CrossRef]
10. Petherick, A. Developing antibody tests for SARS-CoV-2. *Lancet* **2020**, *395*, 1101–1102. [CrossRef]
11. Jiang, S.; Hillyer, C.; Du, L. Neutralizing antibodies against SARS-CoV-2 and other human coronaviruses. *Trends Immunol.* **2020**, *41*, 355–359. [CrossRef]
12. Watson, J.; Richter, A.; Deeks, J. Testing for SARS-CoV-2 antibodies. *BMJ* **2020**, *370*, m3325. [CrossRef]
13. Infantino, M.; Grossi, V.; Lari, B.; Bambi, R.; Perri, A.; Manneschi, M.; Terenzi, G.; Liotti, I.; Ciotta, G.; Taddei, C.; et al. Diagnostic accuracy of an automated chemiluminescent immunoassay for anti-SARS-CoV-2 IgM and IgG antibodies: An Italian experience. *J. Med. Virol.* **2020**, *92*, 1671–1675. [CrossRef] [PubMed]

14. Khan, R.S.; Rehman, I.U. Spectroscopy as a tool for detection and monitoring of coronavirus (COVID-19). *Expert Rev. Mol. Diagn.* **2020**, *20*, 647–649. [CrossRef]
15. Atalan, A. Is the lockdown important to prevent the COVID-9 pandemic? Effects on psychology, environment and economy-perspective. *Ann. Med. Surg.* **2020**, *56*, 38–42. [CrossRef]
16. Peng, G.; Yang, Y.; Pasquarella, J.R.; Xu, L.; Qian, Z.; Holmes, K.V.; Li, F. Structural and molecular evidence suggesting coronavirus-driven evolution of mouse receptor. *J. Biol. Chem.* **2017**, *292*, 2174–2181. [CrossRef]
17. Hoffmann, M.; Kleine-Weber, H.; Schroeder, S.; Krüger, N.; Herrler, T.; Erichsen, S.; Schiergens, T.S.; Herrler, G.; Wu, N.H.; Nitsche, A.; et al. SARS-CoV-2 cell entry depends on ACE2 and TMPRSS2 and is blocked by a clinically proven protease inhibitor. *Cell* **2020**, *181*, 271–280. [CrossRef] [PubMed]
18. Tai, W.; He, L.; Zhang, X.; Pu, J.; Voronin, D.; Jiang, S.; Zhou, Y.; Du, L. Characterization of the receptor-binding domain (RBD) of 2019 novel coronavirus: Implication for development of RBD protein as a viral attachment inhibitor and vaccine. *Cell. Mol. Immunol.* **2020**, *17*, 613–620. [CrossRef] [PubMed]
19. Wrapp, D.; Wang, N.; Corbett, K.S.; Goldsmith, J.A.; Hsieh, C.L.; Abiona, O.; Graham, B.S.; McLellan, J.S. Cryo-EM structure of the 2019-nCoV spike in the prefusion conformation. *Science* **2020**, *367*, 1260–1263. [CrossRef] [PubMed]
20. Wu, F.; Zhao, S.; Yu, B.; Chen, Y.M.; Wang, W.; Song, Z.G.; Hu, Y.; Tao, Z.W.; Tian, J.H.; Pei, Y.Y.; et al. A new coronavirus associated with human respiratory disease in China. *Nature* **2020**, *579*, 265–269. [CrossRef]
21. Gao, Y.; Yan, L.; Huang, Y.; Liu, F.; Zhao, Y.; Cao, L.; Wang, T.; Sun, Q.; Ming, Z.; Zhang, L.; et al. Structure of the RNA-dependent RNA polymerase from COVID-19 virus. *Science* **2020**, *368*, 779–782. [CrossRef] [PubMed]
22. Ekiert, D.C.; Wang, F.; Wilson, I.A.; Schultz, P.G.; Smider, V.V. Reshaping antibody diversity. *Biophys. J.* **2014**, *106*, 438a. [CrossRef]
23. Nguyen, M.N.; Pradhan, M.R.; Verma, C.; Zhong, P. The interfacial character of antibody paratopes: Analysis of antibody-antigen structures. *Bioinformatics* **2017**, *33*, 2971–2976. [CrossRef] [PubMed]
24. Copeland, R.A. Chemical bonds and reactions in biochemistry. In *Enzymes*; 2003; pp. 11–41.
25. Murayama, K.; Tomida, M. Heat-induced secondary structure and conformation change of bovine serum albumin investigated by fourier transform infrared spectroscopy. *Biochemistry* **2004**, *43*, 11526–11532. [CrossRef] [PubMed]
26. Van Stokkum, I.H.M.; Linsdell, H.; Hadden, J.M.; Haris, P.I.; Chapman, D.; Bloemendal, M. Temperature-induced changes in protein structures studied by fourier transform infrared spectroscopy and global analysis. *Biochemistry* **1995**, *34*, 10508–10518. [CrossRef] [PubMed]
27. Kaur, S.P.; Gupta, V. COVID-19 vaccine: A comprehensive status report. *Virus Res.* **2020**, *288*, 198114. [CrossRef] [PubMed]
28. Hume, S.; Hithell, G.; Greetham, G.M.; Donaldson, P.M.; Towrie, M.; Parker, A.W.; Baker, M.J.; Hunt, N.T. Measuring proteins in H2O with 2D-IR spectroscopy. *Chem. Sci.* **2019**, *10*, 6448–6456. [CrossRef]
29. Kitadai, N.; Sawai, T.; Tonoue, R.; Nakashima, S.; Katsura, M.; Fukushi, K. Effects of ions on the OH stretching band of water as revealed by ATR-IR spectroscopy. *J. Solution Chem.* **2014**, *43*, 1055–1077. [CrossRef]
30. Nara, M.; Tasumi, M.; Tanokura, M.; Hiraoki, T.; Yazawa, M.; Tsutsumi, A. Infrared studies of interaction between metal ions and Ca^{2+}-binding proteins Marker bands for identifying the types of coordination of the side-chain COO^{-} groups to metal ions in pike parvalbumin (pI = 4.10). *FEBS Lett.* **1994**, *349*, 84–88. [CrossRef]
31. Yuan, M.; Wu, N.C.; Zhu, X.; Lee, C.C.D.; So, R.T.Y.; Lv, H.; Mok, C.K.P.; Wilson, I.A. A highly conserved cryptic epitope in the receptor binding domains of SARS-CoV-2 and SARS-CoV. *Science.* **2020**, *368*, 630–633. [CrossRef]
32. Liu, J.; Shao, H.; Tao, Y.; Yang, B.; Qian, L.; Yang, X.; Cao, B.; Hu, G.; Tachibana, H.; Cheng, X. Production of an anti-severe acute respiratory syndrome (SARS) coronavirus human monoclonal antibody fab fragment by using a combinatorial immunoglobulin gene library derived from patients who recovered from SARS. *Clin. Vaccine Immunol.* **2006**, *13*, 594–597. [CrossRef]
33. Yuan, M.; Liu, H.; Wu, N.C.; Lee, C.-C.D.; Zhu, X.; Zhao, F.; Huang, D.; Yu, W.; Hua, Y.; Tien, H.; et al. Structural basis of a public antibody response to SARS-CoV-2. *bioRxiv* **2020**. [CrossRef]
34. Chen, W.-H.; Hotez, P.J.; Bottazzi, M.E. Potential for developing a SARS-CoV receptor-binding domain (RBD) recombinant protein as a heterologous human vaccine against coronavirus infectious disease (COVID)-19. *Hum. Vaccines Immunother.* **2020**, *16*, 1239–1242. [CrossRef] [PubMed]
35. Levine, R.D. *Molecular Reaction Dynamics*; Cambridge University Press: Cambridge, UK, 2005; Volume 9780521842, ISBN 9780511614125.
36. Araujo, M.B.; Naimi, B. Spread of SARS-CoV-2 coronavirus likely to be constrained by climate. *medRxiv* **2020**. [CrossRef]
37. Neher, R.A.; Dyrdak, R.; Druelle, V.; Hodcroft, E.B.; Albert, J. Potential impact of seasonal forcing on a SARS-CoV-2 pandemic. *Swiss Med. Wkly.* **2020**, *150*, w20224. [CrossRef] [PubMed]